Hindawi
Advances in Materials Science and Engineering
Volume 2022, Article ID 5136748, 11 pages
https://doi.org/10.1155/2022/5136748

Research Article

Effect of Aromatic Petroleum Resin on Microstructure of SBS Modified Asphalt

Hongjuan Wu,[1] **Peng Chen**,[2] **Chengqin Chen**,[1] **and Wei Zhang**[1]

[1]*School of Civil Engineering, Northwest Minzu University, Lanzhou 730000, China*
[2]*Beijing CCCC Qiaoyu Science and Technology CO.LTD, Beijing 271000, China*

Correspondence should be addressed to Peng Chen; zjqychenpeng1983@yeah.net and Chengqin Chen; cccnmu@126.com

Received 23 February 2022; Accepted 23 March 2022; Published 13 April 2022

Academic Editor: Xiaolong Sun

In this paper, aromatic petroleum resin (APR) was used as raw material. The fluorescence microscopic photography of styrene-butadiene-styrene block copolymer (SBS) modified asphalt with different contents of APR was carried out, and the effect of APR on the dispersion of SBS modified asphalt was quantitatively studied. The nano-surface morphology of SBS modified asphalt with different APR contents was tested by atomic force microscope (AFM), and the effects of APR content on AFM nanoscale parameters such as roughness and maximum amplitude were analyzed. In addition, this paper also tested the basic technical indexes of SBS modified asphalt with different APR contents and revealed its improvement law on the pavement performance of SBS modified asphalt. The results show that the use of APR is beneficial to the shearing of SBS into smaller particles. The larger the amount of APR, the smaller the maximum particle size and average particle size of SBS in asphalt and the smaller the roughness and maximum amplitude of SBS modified asphalt. APR can improve the viscosity and low-temperature ductility of SBS asphalt to a certain extent. High-temperature storage stability is improved obviously; SBS modified asphalt mixed with APR has a more dense spatial cross-linking structure after thorough development. The research results are helpful to reveal the mechanism of APR improving the performance of SBS polymer asphalt.

1. Introduction

SBS modified asphalt is the most widely used polymer asphalt in China, accounting for more than 95% of China's polymer asphalt market. Taking SBS as the main polymer, it has derived the largest polymer asphalt market in the world. SBS is dispersed in asphalt in a swelling state, and the particle size can reach micron level [1]. However, due to the large density gap between SBS and asphalt, the segregation of SBS has been perplexing asphalt production and transportation enterprises. Researchers have tried to use a variety of methods to improve the technical properties of SBS modified asphalt and achieved certain results. Among them, new modifiers are an important way. A variety of materials have been used to improve many technical properties of SBS modified asphalt, such as TiO_2/PS-rGO [2], nano-Al_2O_3 [3], polyphosphoric acid [4], polysulfide regenerant [5], nano-montmorillonite [6], methylene diphenyl diisocyanate [7], multi-dimensional nanomaterials [8], polystyrene grafted activated waste rubber powder [9, 10], oil [11], multi-layered CNTs [12–14], nano-organic palygorskite [15], silica fume [16], and nano-CuO and MWCNT [17].

It can be seen that the use of new modifiers is the mainstream method to improve the technical performance of SBS modified asphalt. In recent years, APR has been used as additives in many fields, and it has good compatibility with asphalt [18–20]. APR refers to a resin material formed by polymerization of olefins or cyclo-olefins containing nine carbon atoms or copolymerization with aldehydes, aromatics, and terpenes [21–24]. APR appears as light yellow to light brown flake or blocks solid, the average molecular weight is 500–1000, the relative density is 0.97–1.04, the softening point is 40-l40°C, the glass transition temperature is 81°C, the refractive index is 1.512, the base value is less than 4, the acid value is less

than 0.1, the bromine value is 7–50, and the iodine value is 30–140 [25, 26]. APR has a ring structure with high cohesion, good acid resistance, chemical resistance, water resistance and weather resistance, but its adhesion is poor. APR has good compatibility with phenolic resin, coumarone resin, polymerized styrene butadiene rubber (SBR), and SBS. It is soluble in acetone, methyl ethyl ketone, cyclohexane, dichloromethane, ethyl acetate, benzene, toluene, and solvent gasoline, but it has poor compatibility with natural rubber and is insoluble in ethanol and water [27–30]. APR is often used as tackifying resins for preparing pressure-sensitive adhesives, hot-melt pressure-sensitive adhesives, and rubber adhesives. Some scholars have also done some related research work on the influence of substances with similar properties to APR on the properties of SBS modified asphalt Zhang W. et al. [31] reported that C9 petroleum resin can improve the storage stability of SBS modified asphalt. Tang et al. [21] revealed that aromatic oil and petroleum resin have good compatibility with SBS, which is conducive to the shear and dispersion of SBS in asphalt. Nie et al. [32] used bio-oil to increase the compatibility between SBS polymer particles and light oil.

In the research methods of SBS modified asphalt, fluorescence microscopy has become an important technology to study SBS modified asphalt. SBS modifier can emit light with a longer wavelength when excited by a short light wave. At present, the acquisition of fluorescent micro-red-green-blue picture (RGB) is relatively mature but still limited to the limitation of interdisciplinary disciplines. When acquiring micro-quantitative parameters, the fixed equal threshold method is generally used to binarize the RGB diagram of SBS modified asphalt. The thickness of each picture is different, which leads to a lot of information being enlarged or reduced, which greatly limits the accuracy of quantitative analysis of the microparameters of SBS modified asphalt by fluorescence microscopy. In addition, AFM technology has become an important means to study asphalt and modified asphalt. Some progress has been made in the measurement method of nano-morphology of asphalt, the relationship between morphology characteristics and macro-mechanical parameters, and the influencing factors of morphology characteristics. However, it is still in its infancy in terms of morphology characteristics and correlation energy. The quantitative analysis of different phases in the asphalt AFM phase diagram will become a breakthrough in this field.

In conclusion, there are not many studies on the action mechanism and effect of APR on SBS modified asphalt. Based on the existing research, this article used APR as the raw material and used a fluorescence microscope to explore its influence on the dispersion of SBS polymer in asphalt. With the help of AFM, the influence law of APR on the nano-surface morphology of SBS modified asphalt was explored, and the technical indexes of APR/SBS modified asphalt were tested. The research results are helpful to reveal the mechanism of APR improving the performance of SBS polymer asphalt.

2. Test Design

2.1. Materials. The KLMY (90#) asphalt used in this article was produced by PetroChina Company Limited (Karamay, China). The technical indexes are shown in Table 1. SBS modifier was produced by Baling Petrochemical Co. Ltd. (Yueyang, China). The technical indexes are shown in Table 2. SBS polymer is used in a 1 : 1 ratio of linear-SBS and star-SBS, and the mixing amount is 4.5% (asphalt mass percentage). The sulfur-based stabilizer was produced by Sichuan Kelutai Transportation Technology Co. Ltd. (Chengdu, China). The technical indexes are shown in Table 3, and the content is 0.2% (percentage of asphalt mass). The APR was produced by Jinan Dahui Chemical Technology Co. Ltd. (Jinan, China), and its technical indexes are shown in Table 4.

The preparation method of SBS modified asphalt used in this paper is as follows. The 90# asphalt is heated to 175°C~185°C, then SBS polymer is added into the asphalt, and the shearing instrument is used to operate at a high speed of 4500 r/min for 50 min. During this period, sulfur-based stabilizers and APR are slowly mixed. After shearing and dispersion, SBS polymer asphalt can be obtained by stirring at 170°C~180°C for 2 h.

2.2. Test Design. In this paper, the quality of SBS in SBS modified asphalt is used as a benchmark, and the content of APR is 0%, 5%, 10%, 15%, and 20%, respectively. The fluorescence microscopic images of SBS polymer asphalt were obtained by fluorescence microscope, and the dispersion effect of APR on SBS in asphalt was analyzed. The nano-surface morphology of SBS polymer asphalt was photographed with the help of the atomic force microscope to study the influence of APR on the nano-morphology of SBS modified asphalt. Finally, the conventional technical properties of APR/SBS modified asphalt were tested.

2.3. Test Specimen Preparation and Test Method

2.3.1. Preparation and Test Method of Fluorescent Micro-Asphalt Specimen. The preparation method of fluorescent micro-asphalt specimen is as follows. Take an appropriate amount of asphalt (2 drops of asphalt in this paper) and drop it on the slide. Put the cover glass on the asphalt. No external force can be applied artificially to prevent the distribution form of polymer in the asphalt from changing due to the intervention of external force. Then, place the slide in the oven at 180°C for 1~2 min to prevent the influence of bubbles in asphalt and uneven cover glass on image quality. The glass slide can be taken out after the asphalt is covered with the cover glass and cooled naturally at 20°C~30°C. If there are many bubbles in the sample, it shall be discarded. Figure 1 is an example of the specimens prepared in this paper and a photo of the fluorescence microscopic test point.

The fluorescence microscope used in this paper is 27C-LQ type produced by Shanghai Putuo Photoelectric Instrument Co. Ltd. When excited by a short wave of light

Table 1: Technical indexes of KLMY 90# asphalt.

Technical indexes		Measured value
Penetration at 25°C, 0.1 mm		88.4
Ductility at 10°C, cm		54.3
Softening point, °C		46.9
RTFOT[1]	Mass change, %	0.42
	Penetration ratio, %	62.7
	Residual ductility at 10°C, cm	14.6

[1]RTFOT: rolling thin film oven test.

Table 2: Technical indexes of SBS.

Technical indexes	Linear-SBS	Star-SBS
S/B	30/70	40/60
Volatile, %	0.6	0.6
Ash, %	0.13	0.15
300% constant tensile stress, MPa	2.1	2.3
Tensile strength, MPa	16.34	8.2
Elongation at break, %	813	573
Permanent set, %	28.5	38.4
Shore hardness, A	76	71
Melt index, g/10 min	1.97	0.86

Table 3: Technical indexes of stabilizer.

Physical form	Proportion	Combustion temperature
Gray black powder	1.4 (25°C)	269°C

Table 4: Technical indexes of APR.

Technical indexes	Measured value
Flash point, °C	260
Kinematic viscosity at 100°C, mm^2/s	14
Ash content, %	0.03
Density, g/cm^3	1.05
Characteristic	Green liquid

wave after the SBS modifier is swelled in asphalt, it can emit light with a longer wavelength, while asphalt and APR do not excite any light. Therefore, the polymer phase and asphalt phase can be clearly distinguished under the fluorescence microscope. Because the fluorescence microscope uses the reflected light field imaging, the real distribution and morphological structure of polymer in asphalt can be clearly observed. In this paper, asphalt specimens are photographed with a fluorescence microscope at 400 times magnification. Asphalt and APR are red, while SBS is yellow. After proofreading, the side length of each fluorescence micrograph is 156 μm.

2.3.2. Preparation and Test Method of AFM Specimen

Preparation Method of AFM Sample. Heat the asphalt to the flowing state, take an appropriate amount of asphalt and drop it on the glass slide (10 drops of asphalt are used in this paper), and then place the glass slide in a horizontal oven at 180°C for 1 min. The asphalt can be basically kept flat without overflow. Then, put the glass slide into the environmental chamber (the carrier remains horizontal) and reduce the asphalt temperature from 180°C to 25°C at a cooling rate of 8°C/min, and the asphalt AFM sample can be successfully prepared. AFM specimens were scanned by atomic force microscope in tap mode at 25°C. The parameters during the AFM test are as follows. The number of samples is 255, the scan size is 10 μm × 10 μm, and the drive amplitude is 300.00 MV. Figure 2 shows the AFM specimen preparation and test process.

3. Results and Discussion

3.1. Effect of APR on the Dispersion of SBS Modifier. Fluorescence microscopic images of undeveloped SBS asphalt were taken. At this time, SBS has become micron fine particles through high-speed shear. However, since the adsorption swelling process of SBS polymer particles on light components in asphalt has not been completed, SBS particles are granular, as shown in Figures 3–7. Figures 3–7 show the fluorescence micrographs of SBS asphalt with different contents of APR.

Figures 3–7 show that the addition of APR has a certain effect on the particle size of SBS particles dispersed in asphalt. The larger the content of APR, the smaller the particle size of SBS. It can be considered that APR is beneficial for SBS to be sheared into finer particles under the condition of the constant shear process.

3.2. Quantitative Analysis of Influence Law of Dispersion Performance. Process the SBS asphalt fluorescence micrograph and unify the pixel size (255 × 200 in this paper); the "imread" command in the MATLAB tool is used to obtain the RGB image of the fluorescence micrograph, and the "im2bw" command is used to obtain the binary image under an appropriate threshold. With the help of the Image-Pro Plus tool, the number of SBS particles and the number of pixels occupied by each SBS particle in the binary image can be counted, and then the area proportion of SBS can be calculated. The particle size, average particle size, maximum particle size, etc. of each SBS particle can also be calculated according to the relationship between the number of pixels and the actual size of the picture. Figure 8 shows an example of a picture processing process.

During the test, the method of increasing the test samples is adopted in order to avoid the influence of the discreteness of a single micro-image on the results. The number of each sample is 5~10, and the representative pictures are shown in Figures 9–13.

The binarization process adopts the processing method of dynamic threshold, and the binarization thresholds of Figures 9–13 are 0.680, 0.751, 0.525, 0.512, and 0.589, respectively. This processing method reduces the problem of the large error caused by using a single threshold in the binarization process of different images and lays a foundation for particle size statistics and image assignment analysis. The particle size distribution of SBS polymer particles with different contents of APR can be observed intuitively in Table 5.

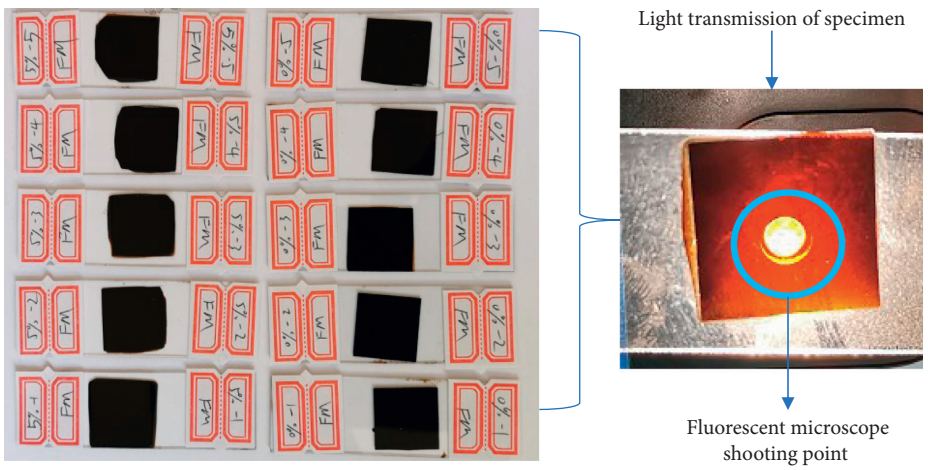

Figure 1: An example of the specimens prepared in this paper and a photo of the fluorescence microscopic test point.

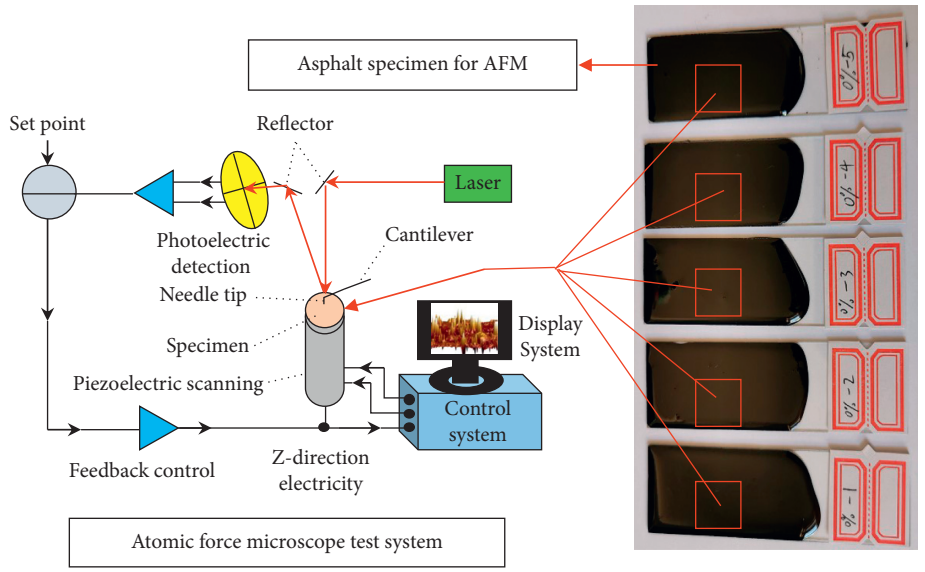

Figure 2: The AFM specimen preparation and test process in this paper.

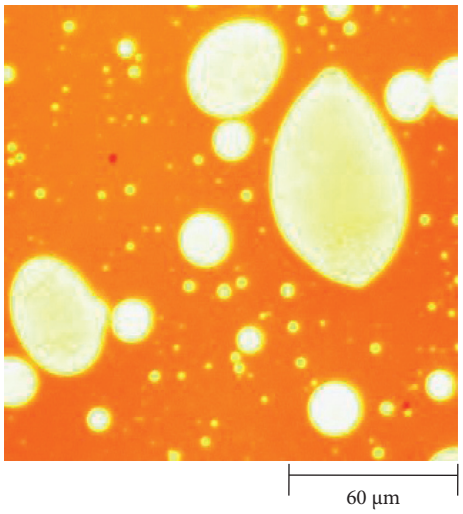

Figure 3: Fluorescence micrographs of undeveloped SBS modified asphalt with 0% content of APR.

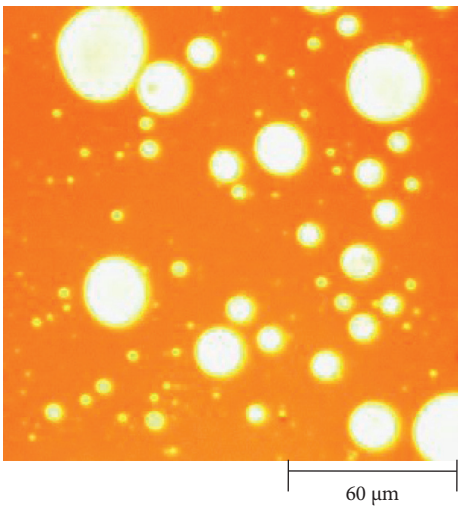

Figure 4: Fluorescence micrographs of undeveloped SBS modified asphalt with 5% content of APR.

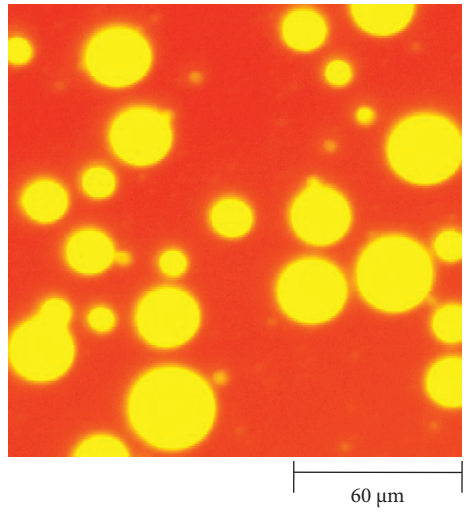

Figure 5: Fluorescence micrographs of undeveloped SBS modified asphalt with 10% content of APR.

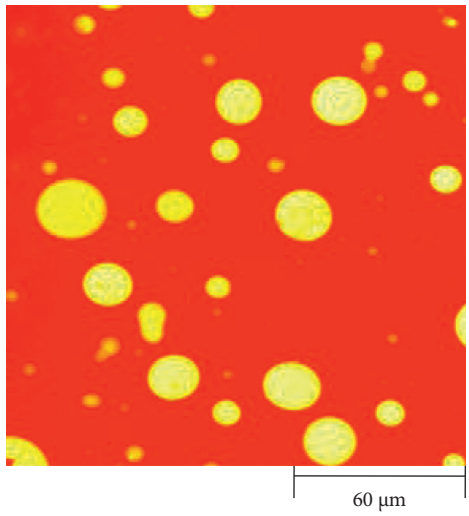

Figure 6: Fluorescence micrographs of undeveloped SBS modified asphalt with 15% content of APR.

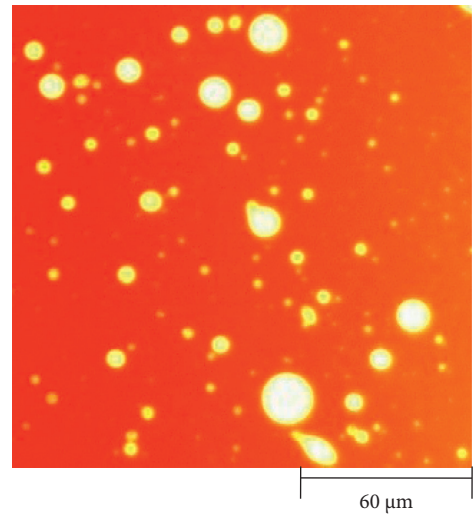

Figure 7: Fluorescence micrographs of undeveloped SBS modified asphalt with 20% content of APR.

Table 5 shows the maximum particle size, average particle size, and area proportion of SBS counted/measured with the help of the Image-Pro Plus tool. From the measurement results, the larger the content of APR, the smaller the maximum particle size and average particle size of SBS modifier particles. Although there is a positive correlation between the area proportion of SBS and the content of APR, the increasing trend is not obvious. The fundamental reason is that the decisive factor of the area proportion of SBS is the content of SBS. Figure 14 shows the test results of the average particle size of SBS polymer with different contents of APR.

Equations (1) and (2) are the calculation equations of the content of APR and the maximum particle size and average particle size of the SBS modifier based on the test results.

$$P_{\max} = 0.157C^2 - 5.867C + 72.84R^2 = 0.934, \quad (1)$$

$$P_{\text{avg}} = -0.40C + 13.08R^2 = 0.965, \quad (2)$$

where $P_{\max}$ is the maximum particle size of SBS modifier, μm; P_{avg} is the average particle size of SBS modifier, μm; C is the content of APR, %; and R is the related coefficient.

Since the APR is a resin substance formed by polymerization of olefins or cycloolefins or copolymerization with aldehydes, aromatics, terpenes, and so on, combined with the research results in Sections 3.1 and 3.2, it can be boldly guessed that the addition of APR makes some substances have a related effect with SBS, which makes the swelling of SBS in asphalt easier and allows it to swell into particles with smaller particle size. As a result, the swelling degree of SBS modified asphalt mixed with APR is much higher.

3.3. Effect of APR on Nano-Morphology of SBS Modified Asphalt

3.3.1. Nanoscale Parameters of Asphalt. The height information of the asphalt surface is collected by AFM, and the scanning results are read by NanoScope Analysis software,

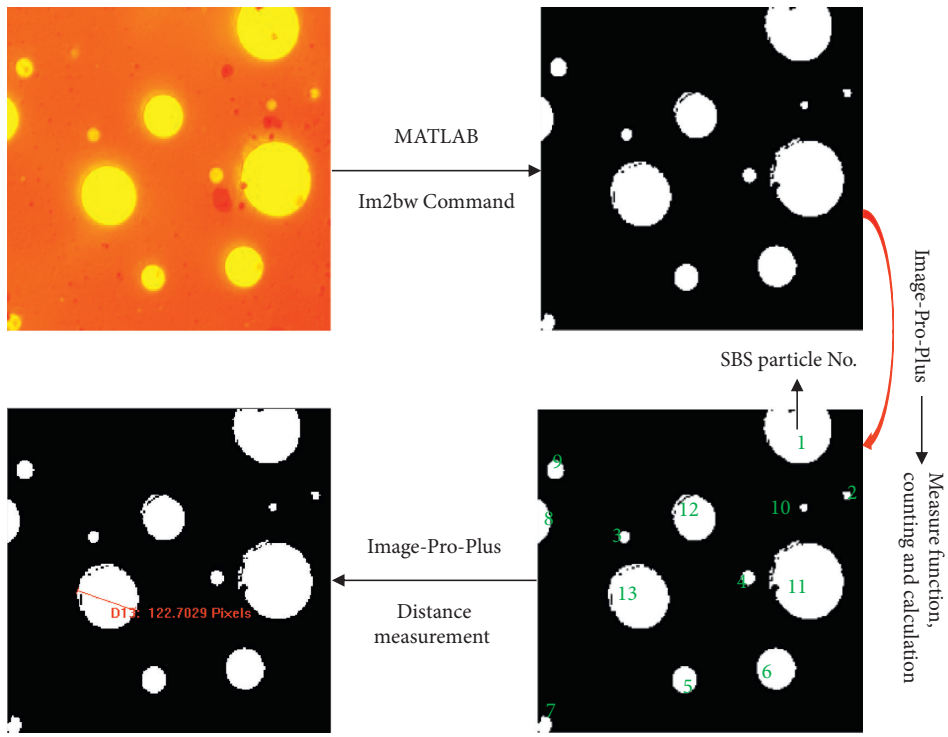

Figure 8: An example of a picture processing process.

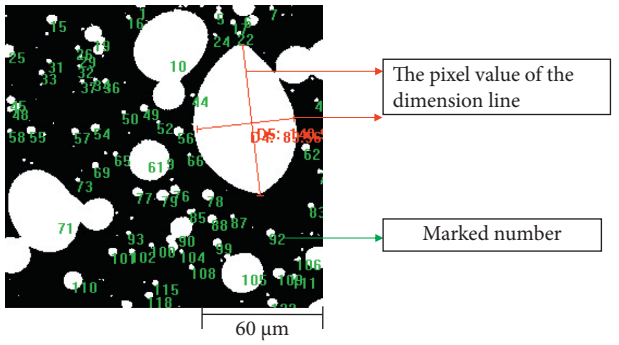

Figure 9: Fluorescence microscopic binarization image of SBS modified asphalt with 0% content of APR.

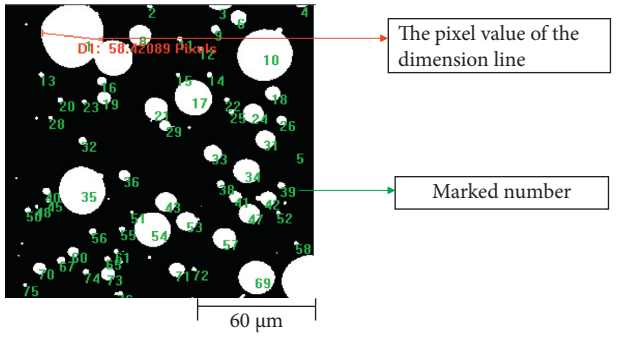

Figure 10: Fluorescence microscopic binarization image of SBS modified asphalt with 5% content of APR.

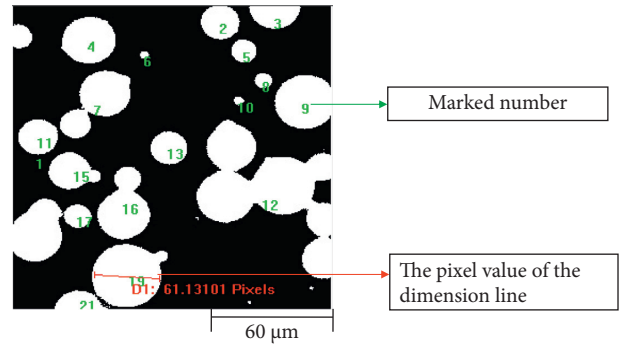

Figure 11: Fluorescence microscopic binarization image of SBS modified asphalt with 10% content of APR.

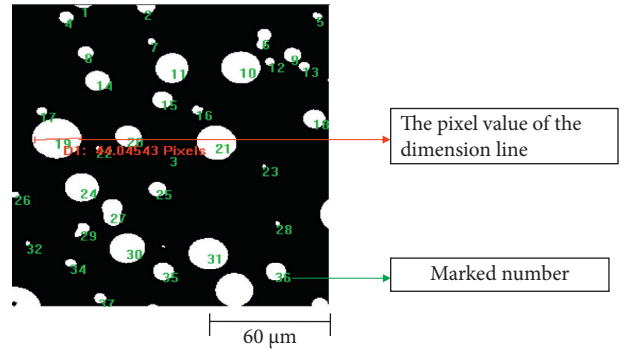

Figure 12: Fluorescence microscopic binarization image of SBS modified asphalt with 15% content of APR.

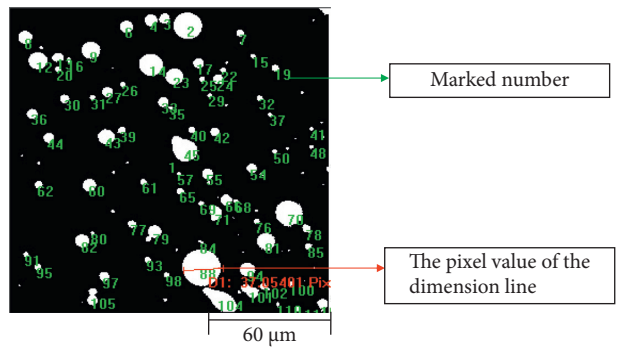

Figure 13: Fluorescence microscopic binarization image of SBS modified asphalt with 20% content of APR.

Table 5: Maximum particle size and average particle size of SBS.

Content of APR, %	Maximum particle size, μm	Average particle size, μm	Proportion of SBS area, %
0	76.8	13.8	9.59
5	37.92	10.2	9.64
10	34.8	9	9.72
15	23.4	7.2	9.79
20	16.2	5.4	9.77

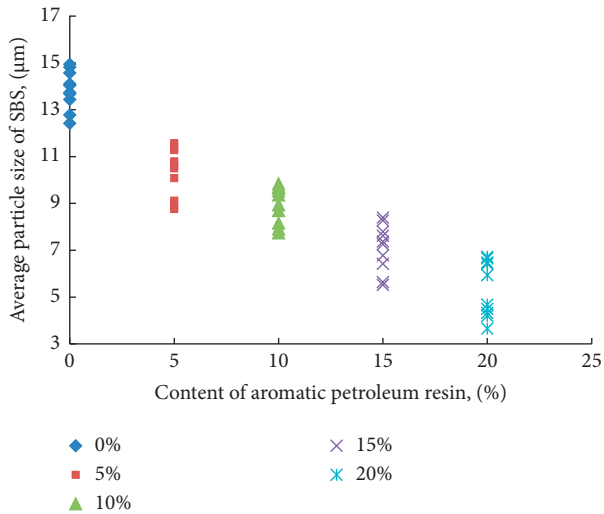

Figure 14: Relationship between average particle size of SBS modifier and content of APR.

and then the roughness value can be automatically calculated.

The roughness selected in this paper is the root mean square roughness (R_q), and the calculation method is shown in the following equation [33, 34]:

$$R_q = \left(\frac{\left(\iint [h(x,y) - h_0]^2 \mathrm{d}A \right)}{\left(\iint \mathrm{d}A \right)} \right)^{1/2}, \quad (3)$$

where A is the scanning area, $10\,\mu\mathrm{m} \times 10\,\mu\mathrm{m}$; $h(x, y)$ is the height function, nm; and h_0 is the reference height, nm, and its calculation method is shown in the following equation [35]:

$$h_0 = \frac{\left(\iint (h(x,y)\mathrm{d}S) \right)}{\left(\iint \mathrm{d}S \right)}. \quad (4)$$

Figure 12 shows the method to obtain the root mean square roughness. The roughness of the selected area can be quickly read by using the roughness module of NanoScope Analysis software.

During the test, it is found that for the same kind of asphalt, under the same test conditions (the cooling rate during forming shall be strictly controlled), the roughness of different test areas (in units of $10\,\mu\mathrm{m} \times 10\,\mu\mathrm{m}$) is relatively stable, and the test error is about 3%. It also provides a guarantee that the roughness can be used as an AFM nanoscale parameter. Figure 15 shows an example of the roughness test method.

This paper defines that the nanoscale parameter (maximum amplitude) based on AFM is the difference between the maximum height ($h_{\max}$) and the minimum height ($h_{\min}$) in the three-dimensional space of height (h). As shown in Figure 16, $h_{\max}$ and $h_{\min}$ can be read or calculated by NanoScope Analysis software. During the test, it is found that for the same kind of asphalt, under the same test conditions (the cooling rate during forming shall be strictly controlled), the maximum amplitude of different test areas (in units of $10\,\mu\mathrm{m} \times 10\,\mu\mathrm{m}$) is relatively stable, and the test error is about 5%. It provides a guarantee that the maximum amplitude can be used as an AFM nanoscale parameter.

3.3.2. Effect of APR Content on Nano-Morphology of SBS Modified Asphalt. In this paper, the AFM specimens of SBS modified asphalt with APR content (SBS mass percentage) of 0%, 5%, 10%, 15%, and 20% were prepared. All tested modified asphalt had been sheared and developed for 2 h. During the preparation of the AFM specimens, the cooling rate of the modified asphalt was controlled at 8°C/min, from 180°C to 25°C, and the scanning of the nano-topography was completed at a temperature of 25°C. There are five groups of data for each content of APR. The nanoscale parameters of

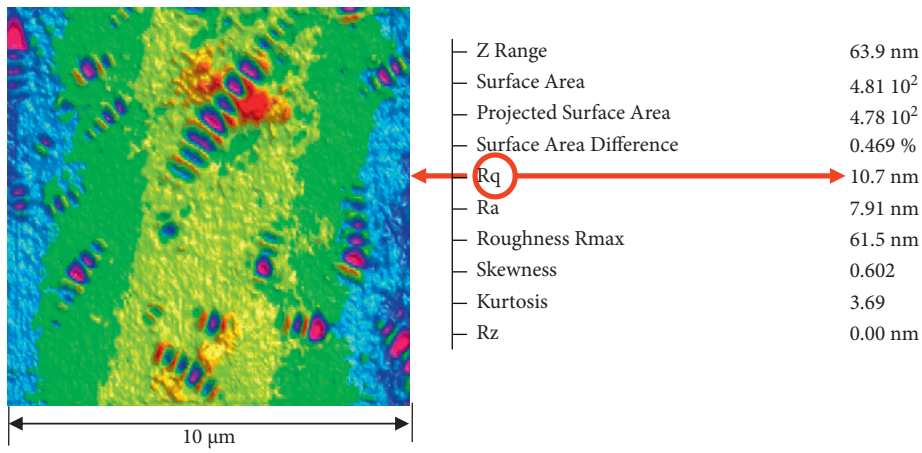

Figure 15: Test method of the roughness.

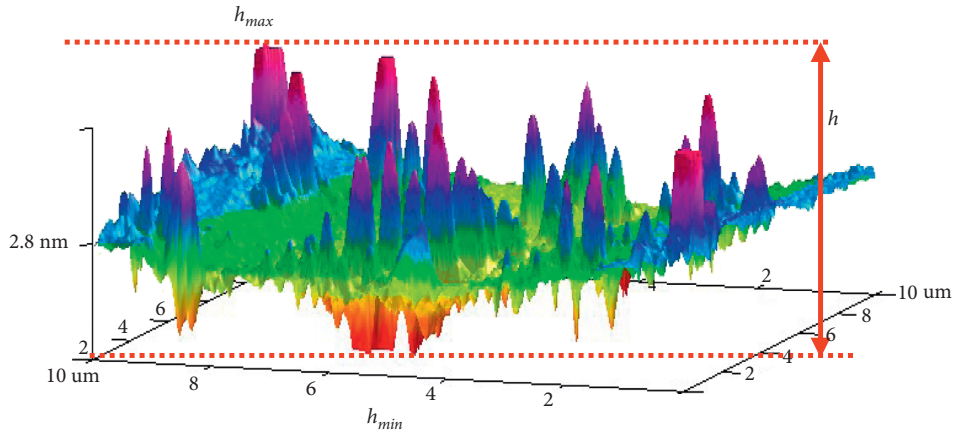

Figure 16: Test method of the maximum amplitude.

SBS modified asphalt with different APR contents are calculated according to the AFM image. The calculation results are shown in Figures 17 and 18.

Figure 17 shows that with the gradual increase in the content of APR, the roughness of SBS modified asphalt shows a gradual decrease trend. When there is no APR, the roughness of SBS modified asphalt is basically maintained at about 9 nm, while when the content of APR reaches 20%, this value is reduced to about 6 nm. These phenomena suggest that APR has a certain interference effect on the formation of the bee-like structure of SBS modified asphalt. Although there is no unified view on the formation reason of bee-like structure, scholars generally believe that roughness, as an index reflecting bee-like structure, has a certain relationship with the technical performance of asphalt. It is generally believed that for the same modified asphalt, the greater the roughness, the stronger the viscosity and the stronger the anti-segregation and anti-ageing performance.

Figure 18 shows the maximum amplitude of SBS modified asphalt with different APR contents. With the continuous increase of the content of APR, the maximum amplitude of SBS modified asphalt shows a gradually decreasing trend, which just reflects the relationship between roughness and the content of APR. When there is no APR, the maximum amplitude of SBS modified asphalt is maintained at about 90 nm, while when the content of APR reaches 20%, this value decreases to about 40 nm, which is very obvious. According to the relevant research, for the same modified asphalt, the maximum amplitude often exists on the bee-like structure, and its numerical value seriously affects the roughness value. Therefore, when the maximum amplitude of asphalt is smaller, the stronger the viscosity is, the stronger the anti-segregation and anti-ageing performance will be.

3.4. Influence of APR on Technical Indexes of SBS Modified Asphalt. After the SBS modified asphalt with different contents of APR was adequately developed, the technical indexes of SBS asphalt with different contents of APR were tested, such as penetration (25°C), 48 h softening point difference, rotational viscosity (135°C), softening point, and ductility (5°C). The test results are summarized in Table 6.

Table 6 shows that softening point, an index of high-temperature viscosity of SBS asphalt, is not sensitive to the use of APR. However, when the amount of APR continues to increase, the penetration, as one of the conditional viscosity indexes of SBS modified asphalt, gradually decreases. At the

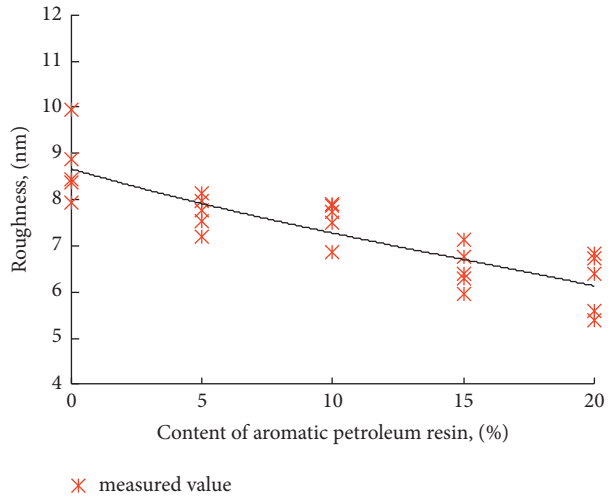

Figure 17: The roughness of SBS modified asphalt with different APR contents.

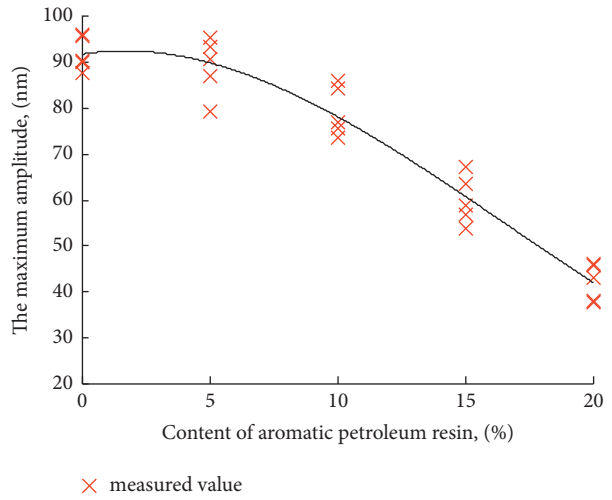

Figure 18: The maximum amplitude of SBS modified asphalt with different APR contents.

Table 6: Technical performance of SBS modified asphalt with different contents of APR.

APR content, %	Penetration at 25°C, 0.1 mm	48 h softening point difference, °C	Viscosity at 135°C, Pa·S	Softening point, °C	Ductility at 5°C, cm
0	65.4	3.4	1.688	80.6	34.6
5	63.5	2.9	1.721	79.5	36.5
10	62.4	2.2	1.796	79.1	37.7
15	61.9	1.6	1.875	80.3	38.4
20	61.2	1.0	1.901	79.5	40.3

same time, the viscosity at 135°C increased significantly, and the ductility at 5°C, an index characterizing the low-temperature ductility of asphalt, also increased. These phenomena indicate that the addition of APR can improve the viscosity and low-temperature performance of SBS modified asphalt.

It is particularly worth mentioning that the 48 h softening point difference of SBS asphalt has changed significantly with the use of APR. When the content of APR is 20%, the value is only 29% when the amount is 0%. This phenomenon shows that the high-temperature storage stability of SBS modified asphalt has been greatly improved by the addition of APR.

This phenomenon can be explained by the micro-image of SBS asphalt after development. Figures 19 and 20 show the fluorescence micrographs when the content of APR is 0% and 20%, respectively.

Figures 19 and 20 show that APR can make SBS polymer easier to be sheared during shearing. SBS particles with small particle sizes have a more thorough swelling state after

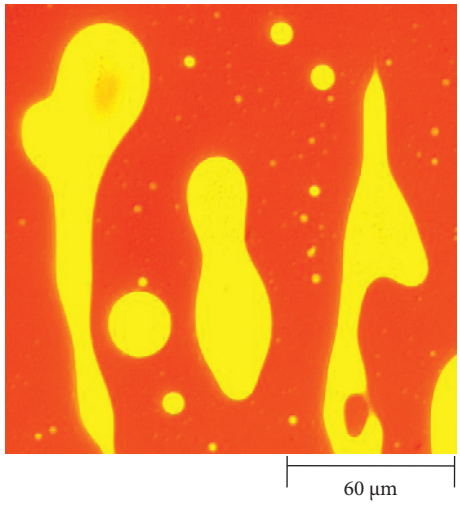

Figure 19: Fluorescence microscopic binarization image of complete development of SBS modified asphalt with 0% content of APR.

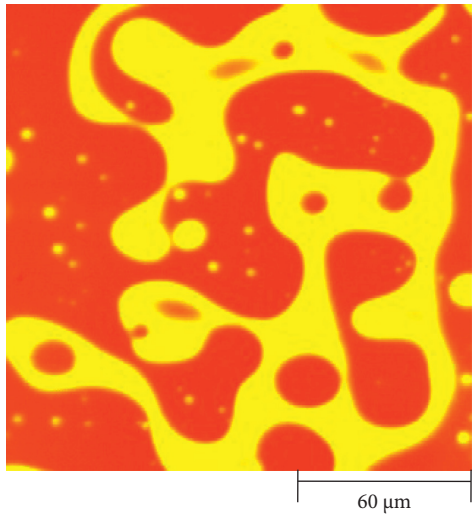

Figure 20: Fluorescence microscopic binarization image of complete development of SBS modified asphalt with 20% content of APR.

thorough development, and the network structure formed by the product of vulcanization reaction with sulfur-based stabilizer is denser. This also explains the differences in technical performance in Table 6.

4. Conclusions

In this paper, based on the existing research, the influence of APR on the dispersion of SBS polymer in asphalt was studied with the help of a fluorescence microscope. With the help of the atomic force microscope, the effect of SBS on the nano-surface morphology of SBS modified asphalt was studied. The technical performance of APR/SBS modified asphalt was tested.

Comparing SBS modified asphalt with different contents of APR, it is found that the larger the content, the smaller the maximum particle size and average particle size of SBS particles. The addition of APR is conducive to the dispersion of SBS into smaller particles in the process of shearing and swelling. AFM test results show that with the increase of the content of APR, the roughness and maximum amplitude of SBS modified asphalt are smaller, indicating that APR also has a significant impact on the nano-morphology of SBS modified asphalt. From the macro-performance test results, APR can improve the viscosity and low-temperature ductility of SBS polymer asphalt to a certain extent and significantly improve the high-temperature storage stability of SBS polymer asphalt.

Data Availability

The data used to support the findings of this study are included within the article.

Conflicts of Interest

The authors declare that they have no conflicts of interest.

Acknowledgments

The authors thank Key Laboratory Base of New Building Materials and Energy-Efficient Building in Gansu Province for providing necessary instruments and equipment for the test. The authors also thank Beijing CCCC Qiaoyu Science and Technology Co. Ltd. for providing all materials for this study free of charge. This study was supported by the Natural Science Foundation of Gansu Province, China (grant no. 17JR5RA288).

References

[1] W. Zhang, F. Wang, J. Shi, Z. Li, and X. Liang, "Experimental study on nano-parameters of styrene-butadiene-styrene block copolymer modified bitumen based on atomic force microscopy," *Polymers*, vol. 11, no. 6, p. 989, 2019.

[2] J. Yang, Y. Muhammad, C. Yang et al., "Preparation of TiO2/PS-rGO incorporated SBS modified asphalt with enhanced resistance against ultraviolet aging," *Construction and Building Materials*, vol. 276, Article ID 121461, 2021.

[3] F. B. Bhat and M. M. Mir, "A study investigating the influence of nano Al2O3 on the performance of SBS modified asphalt binder," *Construction and Building Materials*, vol. 271, Article ID 121499, 2021.

[4] L. Li, Z. Li, Y. Wang, X. Li, and B. Li, "Relation between adhesion properties and microscopic characterization of polyphosphoric acid composite SBS modified asphalt binder," *Frontiers in Materials*, vol. 8, Article ID 633439, 2021.

[5] X. Zhang, X. Zhou, L. Chen, F. Lu, and F. Zhang, "Effects of poly-sulfide regenerant on the rejuvenated performance of SBS modified asphalt-binder," *Molecular Simulation*, vol. 47, no. 17, pp. 1423–1432, 2021.

[6] F. Ye, W. Yin, H. Lu, and Y. Dong, "Property improvement of Nano-Montmorillonite/SBS modified asphalt binder by naphthenic oil," *Construction and Building Materials*, vol. 243, Article ID 118200, 2020.

[7] J. H. Ting, E. Khare, A. DeBellis et al., "Role of methylene diphenyl diisocyanate (MDI) additives on SBS-modified asphalt with improved thermal stability and mechanical

performance," *Energy & Fuels*, vol. 35, no. 21, Article ID 17641, 2021.

[8] Z. Chen, D. Zhang, Y. Zhang, H. Zhang, and S. Zhang, "Influence of multi-dimensional nanomaterials composite form on thermal and ultraviolet oxidation aging resistances of SBS modified asphalt," *Construction and Building Materials*, vol. 273, Article ID 122054, 2021.

[9] B. Liu, J. Li, M. Han, Z. Zhang, and X. Jiang, "Properties of polystyrene grafted activated waste rubber powder (PS-ARP) composite SBS modified asphalt," *Construction and Building Materials*, vol. 238, Article ID 117737, 2020.

[10] C. Qian and W. Fan, "Evaluation and characterization of properties of crumb rubber/SBS modified asphalt," *Materials Chemistry and Physics*, vol. 253, Article ID 123319, 2020.

[11] J. Xu, J. Pei, J. Cai, T. Liu, and Y. Wen, "Performance improvement and aging property of oil/SBS modified asphalt," *Construction and Building Materials*, vol. 300, Article ID 123735, 2021.

[12] X. Zhang, X. Zhou, W. Ji, F. Zhang, and F. Otto, "Characterizing the mechanical properties of Multi-Layered CNTs reinforced SBS modified Asphalt-Binder," *Construction and Building Materials*, vol. 296, Article ID 123658, 2021.

[13] R. Wang, M. Yue, Y. Xiong, and J. Yue, "Experimental study on mechanism, aging, rheology and fatigue performance of carbon nanomaterial/SBS-modified asphalt binders," *Construction and Building Materials*, vol. 268, Article ID 121189, 2021.

[14] X. Zheng, W. Xu, and S. Xie, "Study on ultraviolet aging mechanism of carbon nanotubes/SBS composite-modified asphalt in two-dimensional infrared correlation spectroscopy," *Materials*, vol. 14, no. 19, p. 5672, 2021.

[15] S. Liu, Y. Gao, J. Jin et al., "Synergy effect of nano-organic palygorskite on the properties of star-shaped SBS-modified asphalt," *Polymers*, vol. 13, no. 6, p. 863, 2021.

[16] X. Zheng, W. Xu, H. Feng, and K. Cao, "High and low temperature performance and fatigue properties of silica fume/SBS compound modified asphalt," *Materials*, vol. 13, no. 19, p. 4446, 2020.

[17] N. Amini, H. Latifi, and P. Hayati, "Effects of nano-CuO, MWCNT and SBS on the aging of asphalt binder: FTIR and XRD analyses," *Jordan Journal of Civil Engineering*, vol. 15, pp. 277–291, 2021.

[18] M. Elkashef, M. D. Elwardany, Y. Liang et al., "Effect of using rejuvenators on the chemical, thermal, and rheological properties of asphalt binders," *Energy & Fuels*, vol. 34, no. 2, pp. 2152–2159, 2020.

[19] T. Wang, T. Yi, and Z. Yuzhen, "The compatibility of SBS-modified asphalt," *Petroleum Science and Technology*, vol. 28, no. 7, pp. 764–772, 2010.

[20] Z. Liu, M. Xuan, Z. Zhao, Y. Cong, and K. Liao, "A study of the compatibility between asphalt and SBS," *Petroleum Science and Technology*, vol. 21, no. 7-8, pp. 1317–1325, 2003.

[21] P. Tang, L. Mo, C. Pan, H. Fang, B. Javilla, and M. Riara, "Investigation of rheological properties of light colored synthetic asphalt binders containing different polymer modifiers," *Construction and Building Materials*, vol. 161, pp. 175–185, 2018.

[22] A. V. Morozova and G. I. Volkova, "Effect of the petroleum resin structure on the properties of a petroleum-like system," *Petroleum Chemistry*, vol. 59, no. 10, pp. 1153–1160, 2019.

[23] M. I. L. Abutaqiya, A. A. AlHammadi, C. J. Sisco, and F. M. Vargas, "Aromatic ring index (ari): a characterization factor for nonpolar hydrocarbons from molecular weight and refractive index," *Energy & Fuels*, vol. 35, no. 2, pp. 1113–1119, 2021.

[24] E. Kraus, L. Orf, V. Sitnik et al., "Composition and surface energy characteristics of new petroleum resins," *Polymer Engineering & Science*, vol. 57, no. 9, pp. 1028–1032, 2017.

[25] M. Mousavi, T. Abdollahi, F. Pahlavan, and E. H. Fini, "The influence of asphaltene-resin molecular interactions on the colloidal stability of crude oil," *Fuel*, vol. 183, pp. 262–271, 2016.

[26] M. Lashkarbolooki and S. Ayatollahi, "Effects of asphaltene, resin and crude oil type on the interfacial tension of crude oil/brine solution," *Fuel*, vol. 223, pp. 261–267, 2018.

[27] I. A. Sizova, D. I. Panyukova, and A. L. Maksimov, "Hydrotreating of high-aromatic waste of coke and by-product processes in the presence of in situ synthesized sulfide nanocatalysts," *Petroleum Chemistry*, vol. 57, no. 14, pp. 1304–1309, 2017.

[28] E. Kraus, L. Orf, I. Starostina, A. Efimova, R. Perelygina, and O. Stoyanov, "Composite materials based on polyolefins with new petroleum resins," *Polymer Engineering & Science*, vol. 58, no. 12, pp. 2288–2292, 2018.

[29] A. A. Grin'ko, R. S. Min, T. A. Sagachenko, and A. K. Golovko, "Aromatic sulfur-containing structural units of resins and asphaltenes in heavy hydrocarbon feedstock," *Petroleum Chemistry*, vol. 52, no. 4, pp. 221–227, 2012.

[30] I. N. Frolov, T. N. Yusupova, M. A. Ziganshin, E. S. Okhotnikova, and A. A. Firsin, "Interpretation of thermal effects in differential scanning calorimetry study of asphalts," *Petroleum Chemistry*, vol. 58, no. 8, pp. 593–598, 2018.

[31] W. Zhang, L. Qiu, J. Liu et al., "Modification mechanism of C9 petroleum resin and its influence on SBS modified asphalt," *Construction and Building Materials*, vol. 306, Article ID 124740, 2021.

[32] X. Nie, Z. Li, H. Yao, T. Hou, X. Zhou, and C. Li, "Waste bio-oil as a compatibilizer for high content SBS modified asphalt," *Petroleum Science and Technology*, vol. 38, no. 4, pp. 316–322, 2020.

[33] W. Zhang, L. Zou, Z. Jia, F. Wang, Y. Li, and P. Shi, "Effect of thermo-oxidative ageing on nano-morphology of bitumen," *Applied Sciences*, vol. 9, no. 15, p. 3027, 2019.

[34] T. Su, T. Wang, C. Wang, and H. Yi, "The influence of salt-frost cycles on the bond behavior distribution between rebar and recycled coarse aggregate concrete," *Journal of Building Engineering*, vol. 45, Article ID 103568, 2022.

[35] Ž. Jelčić, V. O. Bulatović, K. J. Marković, and V. Rek, "Multifractal morphology of un-aged and aged SBS polymer-modified bitumen," *Plastics, Rubber and Composites*, vol. 46, no. 2, pp. 77–98, 2017.